

A New Method for Impulse Noise Elimination and Edge Preservation

Une nouvelle méthode pour l'élimination du bruit impulsif et la préservation des contours

Zayed M. Ramadan, *Member, IEEE*

Abstract—In this paper, a new method for impulsive noise reduction and edge preservation in images is presented. Images of different characteristics corrupted with a wide range of impulsive noise densities using two impulsive noise models are examined using the proposed method. In the detection stage of the method, two conditions have to be met to determine whether an image pixel is noisy or not. Two predetermined threshold values are involved in the computation of the second condition to differentiate between corrupted and uncorrupted pixels. Only pixels determined to be noisy in the detection stage are filtered in the next filtering stage where small size sliding windows are used to significantly reduce blurring effects in the output restored images. Several measuring indices have been used to examine the performance of the proposed method compared with many existing state-of-the-art methods in the literature of the image restoration field. Extensive simulation results show the superior performance of the proposed method over other techniques in terms of restoration quality, and preservation of images with fine details and edges.

Résumé—Dans cet article, une nouvelle méthode est présentée pour la réduction du bruit impulsif et la préservation des contours dans une image. Des images ayant différentes caractéristiques altérées avec une densité très variée de deux modèles de bruit impulsif sont étudiées en utilisant la méthode proposée. Durant la phase de détection de notre méthode, deux conditions doivent être satisfaites pour déterminer si un pixel de l'image est bruité. Deux seuils pré-déterminés sont utilisés dans le calcul de la deuxième condition pour différencier les pixels endommagés de ceux qui ne le sont pas. Par la suite, uniquement les pixels marqués comme bruités durant la phase de détection sont filtrés où des fenêtres coulissantes de petite taille sont utilisées pour réduire de manière significative les effets de flou dans les images restaurées obtenues. Plusieurs mesures de performances ont été utilisées pour analyser le rendement de la méthode proposée par rapport à d'autres méthodes déjà publiées dans le domaine de la restauration d'image. Les résultats de plusieurs simulations montrent que la performance de la méthode proposée est supérieure aux autres techniques par rapport à la qualité de la restauration et la conservation des petits détails et contours des images.

Index Terms—Image filtering, median filtering, noise detection, noise suppression, salt-and-pepper noise.

I. INTRODUCTION

IMAGE restoration is one of the main research areas in digital image processing that aims to improve the degraded image by removing the noise corrupting it while preserving its features and details intact [1], [2]. This process of denoising is often based on a probabilistic model of the noise that corrupts the image. One of the common types of noise is impulsive noise that occurs due to noisy sensors and communication channels.

In the literature of digital image processing, many methods have been proposed over the years to solve the problem of image degradation due to impulsive noise. Median filters are

among the most popular image filtering techniques used to eliminate this noise. The main idea in standard median filtering (SMF) is to slide a square window of length $(2k + 1)$ over the entire image and replace the central pixel in the window by the median value of all the pixels in the same window. The effective noise suppression obtained using this method is accompanied by blurred and distorted features, thus loosing image fine details and edges.

Variants of median filters have evolved in image processing research to improve the restored output image. In particular, these methods apply filtering only on the pixels which are detected in a previous stage to be noisy pixels. Therefore, the detection stage in these modified median filtering methods plays a major role in their performance.

A tri-state median filter that incorporates the SFM and the center weighted median (CWM) filter [3] is proposed in [4]. A progressive switching median (PSM) filter is introduced in [5]. To ensure image noise removal in the PSM filter, both detection and filtering stages are progressively applied through several iterations. An algorithm that uses the alpha-trimmed mean (ATM) approach, which is a special case of order-statistics filter, is proposed in [6].

Manuscript received October 30, 2013; revised December 26, 2013; accepted February 5, 2014. Date of current version April 16, 2014. This work was supported by the Deanship of Scientific Research (DSR) at King Abdulaziz University, Jeddah, Saudi Arabia.

The author is with the Electrical and Computer Engineering Department, King Abdulaziz University, North Jeddah Campus, Jeddah 21589, Saudi Arabia (e-mail: zayedr@ieee.org).

Associate Editor managing this paper's review: Farzad Khalvati.

Color versions of one or more of the figures in this paper are available online at <http://ieeexplore.ieee.org>.

Digital Object Identifier 10.1109/CJECE.2014.2309071

A modified switching median filter is introduced in [7] where the detection stage is designed based on the rank-order statistics of the pixels in the sliding window. An algorithm that uses the fuzzy impulse detection (FID) technique is employed in [8]. Cost function minimization (CFM) is used in [9] to remove impulse noise and outliers.

An adaptive CMW (ACWM) filter proposed in [10] is based on estimate calculations of the differences between the outputs of CWM filters and the current pixel under consideration in the sliding window. The detection stage in [11] uses a specialized regularization technique to remove salt and pepper noise.

A differential rank impulse detector (DRID) that compares signal samples within a narrow rank window based on both the rank and absolute value is proposed in [12]. In [13], the corrupted pixels are replaced by either the median pixel or neighborhood pixel depending on a decision-based algorithm (DBA) using a small fixed size (3×3) sliding window.

A convolution-based impulse detector and switching median filter (CD-SMF) algorithm is proposed in [14]. Similarly, the image restoration scheme shown in [15] is based on the computation of the minimum absolute value (MAV) of four convolutions using 1-D Laplacian operator.

In these methods, the pixels declared as noisy can in fact belong to the set of some flat regions in the image, which are uncorrupted pixels. Moreover, these methods do not produce pleasing performance in terms of preservation of image sharpness, edges, and details, mainly for images with different features and high noise densities. To solve these problems, a new method is proposed in this paper in which some conditions are added in the detection stage for more investigation and validation of pixels to determine whether they are noisy or not. The proposed method uses two salt-and-pepper impulsive noise models that are more realistic in practical applications, and uses several images of different characteristics.

This paper is organized and presented as follows. The proposed method is illustrated in Section II, extensive simulation results are depicted and analyzed in Section III, and the conclusion is shown in Section IV.

II. PROPOSED METHOD

The noise type considered in this paper is more realistic and general than the well-known fixed valued impulsive noise that takes a value of 0 or 255 (salt and pepper noise). This noise can be implemented using two classified models as shown below [16]. In these two models, the impulsive noise is represented by two equal intervals at the beginning (pepper) and at the end (salt) of the dynamic range of image intensity values. These values at both ends are randomly distributed throughout the corrupted image.

A. Noise Model 1

In this model, the probability density function of $x_{i,j}$, ie., $f(x_{i,j})$, can be expressed as

$$f(x_{i,j}) = \begin{cases} p/2, & 0 \leq x_{i,j} < m \\ 1-p, & x_{i,j} = s_{i,j} \\ p/2, & 255 - m < x_{i,j} \leq 255 \end{cases} \quad (1)$$

where $x_{i,j}$ is the (i, j) th pixel in the corrupted image, $s_{i,j}$ is the (i, j) th pixel in the original image, and p is the noise density. The dynamic range of an image intensity values is $[0 L - 1]$, where $L = 2^n$ and n is the number of bits per pixel (also called bit depth). In (1), an 8-bit gray image is assumed and hence, $n = 8$ and $L = 256$.

B. Noise Model 2

In this model, the noise probabilities of pepper noise and salt noise are different ($p_1 \neq p_2$)

$$f(x_{i,j}) = \begin{cases} p_1, & 0 \leq x_{i,j} < m \\ 1-p, & x_{i,j} = s_{i,j} \\ p_2, & 255 - m < x_{i,j} \leq 255 \end{cases} \quad (2)$$

where $p = (p_1 + p_2)$ and p_1 and p_2 represent the pepper and salt noise densities, respectively. Having p_1 greater than p_2 , for example, indicates that pepper noise is more probabilistic than salt noise in the corrupted image.

The proposed method is designed to suppress the impulsive noise while preserving image details with minimum blurring, mainly in images having some flat regions through its edges and details, and in those subjected to unequal amounts of pepper and salt noise.

The proposed method in this paper consists of two stages: detection and filtering. In the detection stage, a pixel in the corrupted image $x_{i,j}$ is considered noisy if two conditions are satisfied.

1) *First Condition:* $0 \leq x_{i,j} < m$ or $(255 - m) < x_{i,j} \leq 255$, which can be expressed as

$$\text{Class}_1(x_{i,j}) = \begin{cases} \text{Pepper Noise}, & 0 \leq x_{i,j} < m \\ \text{Salt Noise}, & (255 - m) < x_{i,j} \leq 255 \\ \text{Uncorrupted}, & \text{Otherwise.} \end{cases} \quad (3)$$

2) *Second Condition:* If the number of pixels in the sliding window that belongs to the m_1 -length interval $[0 m_1]$ is called N_1 , and the number of pixels in the sliding window that belongs to the m_2 - length interval $(255 - m_2 255]$ is called N_2 , then the second condition that must also be satisfied for a pixel to be classified as noisy is

$$\text{Class}_2(x_{i,j}) = \begin{cases} \text{Pepper Noise}, & N_1 \leq \alpha_1 \\ \text{Salt Noise}, & N_2 \leq \alpha_2 \\ \text{Uncorrupted}, & \text{Otherwise} \end{cases} \quad (4)$$

where α_1 and α_2 are two thresholds whose values are mainly dependent on noise densities and image characteristics. These two thresholds are directly proportional to the noise density, and are less than or equal to the total number of elements in the sliding window, i.e., $\alpha_1 \leq W^2$ and $\alpha_2 \leq W^2$, where W is the length of the square filtering window.

Only pixels that have been detected to be noisy through validation of the above two conditions are filtered in the second stage. The remaining pixels (uncorrupted ones) are kept unchanged. The size of the square sliding window is dependent on the total noise density. Extensive simulations of the proposed method performed on a large number of images of different characteristics show that small square sliding



Fig. 1. Tested images. From left to right: first row: *Lena*, *Woman*, and *Mandrill*; second row: *Bridge*, *Mammogram*, and *Compound Eye of Fly*.

window lengths W produce the best results in terms of noise suppression and preservation of image fine details and edges. The following roughly estimate values of W were used in the simulations of the proposed method in which up to $p = 60\%$ total noise density is considered

$$W = \begin{cases} 3, & p < 0.5 \\ 5, & 0.5 \leq p \leq 0.6. \end{cases} \quad (5)$$

To find an estimate for the noise density \tilde{p} in the case where pepper and salt have equal probabilities, the following formula can be used as a starting estimate value after which the most optimum value can be found through experimental simulations:

$$\tilde{p} = \frac{K}{MN} \quad (6)$$

where K is the total number of zeros and 255 s in the corrupted image, and the product MN is the total number of pixels in that image.

For different pepper and salt noise densities (p_1 and p_2 , respectively), similar estimates (\tilde{p}_1 and \tilde{p}_2) can be directly concluded as follows:

$$\tilde{p}_1 = \frac{K_1}{MN} \quad (7)$$

$$\tilde{p}_2 = \frac{K_2}{MN} \quad (8)$$

where K_1 and K_2 are the number of zeros and 255s in the corrupted image, respectively.

The most optimum values of the thresholds, α_1 and α_2 , can be computed through computer simulations. However,

starting good estimates for these thresholds can be calculated as follows:

$$\alpha_1 = \begin{cases} \lfloor W^2(\tilde{p}_1 + 0.50) \rfloor & W = 3 \\ \lfloor W^2(\tilde{p}_1 + 0.15) \rfloor & W = 5 \end{cases} \quad (9)$$

$$\alpha_2 = \begin{cases} \lfloor W^2(\tilde{p}_2 + 0.50) \rfloor & W = 3 \\ \lfloor W^2(\tilde{p}_2 + 0.15) \rfloor & W = 5 \end{cases} \quad (10)$$

where $\lfloor \cdot \rfloor$ is the floor operation.

Objective measures are commonly used to evaluate the image restoration quality, i.e., the closeness between the restored image and the original uncorrupted image, and the detail preservation capabilities. In this paper, the mean absolute error (MAE) and the peak signal-to-noise ratio (PSNR) in dB are used. These measuring indices are defined as follows:

$$\text{MAE} = \frac{1}{MN} \sum_{i=1}^M \sum_{j=1}^N |R_{i,j} - U_{i,j}| \quad (11)$$

$$\text{PSNR} = 10 \log_{10} \frac{(L-1)^2}{\frac{1}{MN} \sum_{i=1}^M \sum_{j=1}^N (R_{i,j} - U_{i,j})^2} \quad (12)$$

where $L = 256$ for 8-bit gray scale images, M and N are the total number of pixels in the horizontal and vertical dimensions of the image, and $R_{i,j}$ and $U_{i,j}$ are the pixel values in the (i, j) th locations of the restored (filtered) image and the uncorrupted image, respectively.

Since it has been shown by many researchers that PSNR and MAE are inconsistent with the eye perception, an alternative index called structural similarity (SSIM) index was

TABLE I
PERFORMANCE MEASURE OF THE PROPOSED METHOD USING NOISE MODEL 1 WITH $m = 4$

	p	α_1	α_2	MAE_o	MAE	$PSNR_o$	$PSNR$	$SSIM_o$	$SSIM$
Lena image	10%	7	7	12.56	0.37	15.56	42.62	0.4041	0.9978
	30%	8	8	37.83	1.17	10.76	37.16	0.2015	0.9914
	60%	19	19	75.64	3.22	7.75	30.86	0.0878	0.9604
Woman image	10%	5	5	12.60	0.37	14.10	43.37	0.3253	0.9973
	30%	7	7	37.80	1.08	9.32	38.38	0.1563	0.9914
	60%	19	19	75.67	2.26	6.31	34.61	0.0715	0.9816
Mandrill image	10%	7	7	12.63	0.64	15.69	38.47	0.5742	0.9971
	30%	8	8	37.76	2.08	10.94	33.02	0.2951	0.9864
	60%	19	19	75.63	7.00	7.92	25.76	0.1142	0.8946
Bridge image	10%	7	7	12.57	0.88	15.44	35.74	0.5682	0.9946
	30%	8	8	37.82	2.75	10.65	30.59	0.2968	0.9787
	60%	18	18	75.63	7.20	7.64	25.59	0.1165	0.8987
Mam. image	10%	5	5	12.61	0.61	13.95	36.38	0.1585	0.9801
	30%	7	7	38.18	1.63	9.12	32.30	0.0417	0.9377
	60%	19	19	76.23	3.91	6.12	27.89	0.0134	0.8198
Fly Eye image	10%	5	5	12.59	0.44	14.56	38.46	0.5046	0.9986
	30%	6	6	37.79	1.25	9.77	32.04	0.2797	0.9896
	60%	16	16	75.73	4.23	6.75	26.31	0.1209	0.9541

TABLE II
PERFORMANCE MEASURE OF THE PROPOSED METHOD USING NOISE MODEL 2 WITH $m = 4$

	p_1	p_2	p	α_1	α_2	MAE_o	MAE	$PSNR_o$	$PSNR$	$SSIM_o$	$SSIM$
Lena image	4%	6%	10%	6	6	12.69	0.37	15.48	42.58	0.4054	0.9987
	6%	4%	10%	6	6	12.54	0.37	15.57	42.52	0.4090	0.9987
	10%	20%	30%	7	8	38.01	1.17	10.72	37.04	0.2003	0.9906
	20%	10%	30%	8	7	37.38	1.18	10.85	37.03	0.2089	0.9912
	20%	40%	60%	15	21	76.24	3.22	7.69	30.83	0.0888	0.9605
	40%	20%	60%	21	15	74.88	3.24	7.83	30.81	0.0942	0.9605
Bridge image	4%	6%	10%	6	7	12.85	0.88	15.28	35.71	0.5623	0.9945
	10%	20%	30%	7	8	38.95	2.75	10.43	30.59	0.2914	0.9790
	20%	40%	60%	15	19	78.03	7.21	7.41	25.56	0.1224	0.8984
Mam. image	4%	6%	10%	3	5	14.43	0.56	13.22	35.61	0.1431	0.9825
	10%	20%	30%	5	8	46.18	1.55	8.13	32.57	0.0361	0.9468
	20%	40%	60%	12	22	92.48	3.73	5.11	28.32	0.0117	0.8333
Fly Eye image	4%	6%	10%	4	5	13.64	0.41	14.07	38.94	0.4867	0.9988
	6%	4%	10%	5	4	11.68	0.42	15.00	38.64	0.5222	0.9981
	10%	20%	30%	5	6	43.01	1.25	9.01	31.95	0.2687	0.9865
	20%	10%	30%	6	5	32.71	1.21	10.68	32.49	0.3078	0.9923
	20%	40%	60%	12	18	85.81	4.24	6.01	26.25	0.1227	0.9510
	40%	20%	60%	18	12	65.43	4.26	7.66	26.34	0.1382	0.9479

found to improve the images quality measure. The SSIM index measures the similarity between the two images. If the two images are identical, then $SSIM = 1$, and if they are very dissimilar then the SSIM will be close to zero. For two images, x and y , the SSIM index is defined

as [17]–[20]

$$SSIM(x, y) = [l(x, y)]^\alpha \cdot [c(x, y)]^\beta \cdot [s(x, y)]^\gamma \quad (13)$$

where $l(x, y)$, $c(x, y)$, and $s(x, y)$ are the luminance, contrast and structure components, respectively, of the index.

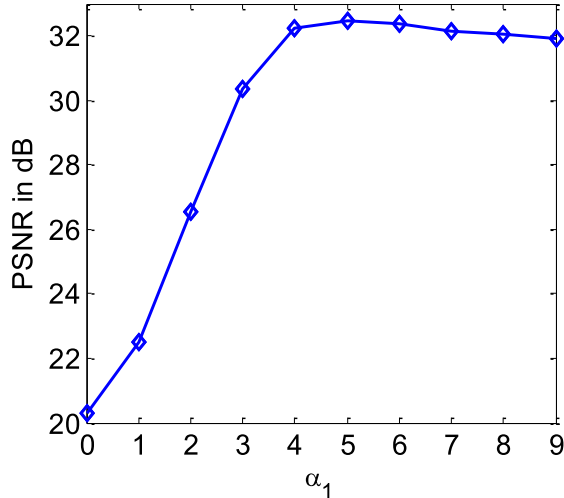


Fig. 2. PSNR versus α_1 in the proposed method using Mammogram image with $W = 3$, $\alpha_2 = 8$ and $p = 30\%$ ($p_1 = 10\%$, $p_2 = 20\%$).

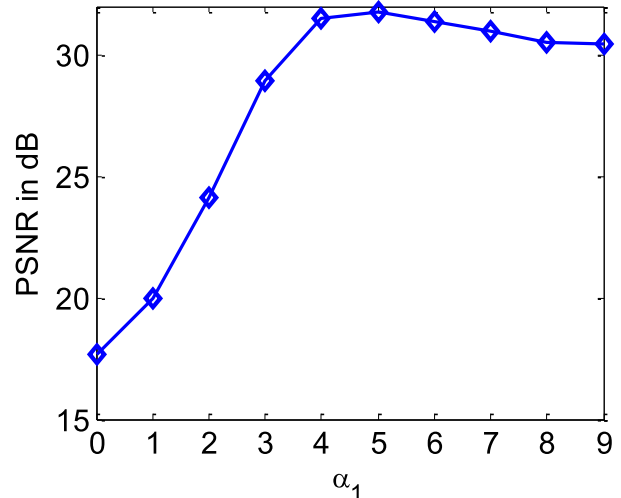


Fig. 4. PSNR versus α_1 in the proposed method using Fly Eye image with $W = 3$, $\alpha_2 = 6$ and $p = 30\%$ ($p_1 = 10\%$, $p_2 = 20\%$).

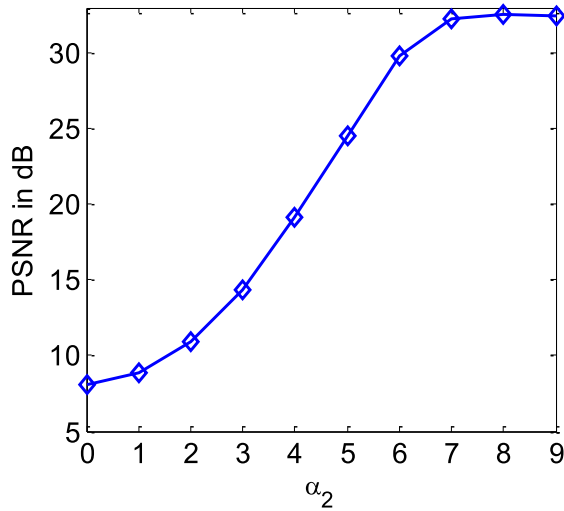


Fig. 3. PSNR versus α_2 in the proposed method using Mammogram image with $W = 3$, $\alpha_1 = 5$ and $p = 30\%$ ($p_1 = 10\%$, $p_2 = 20\%$).

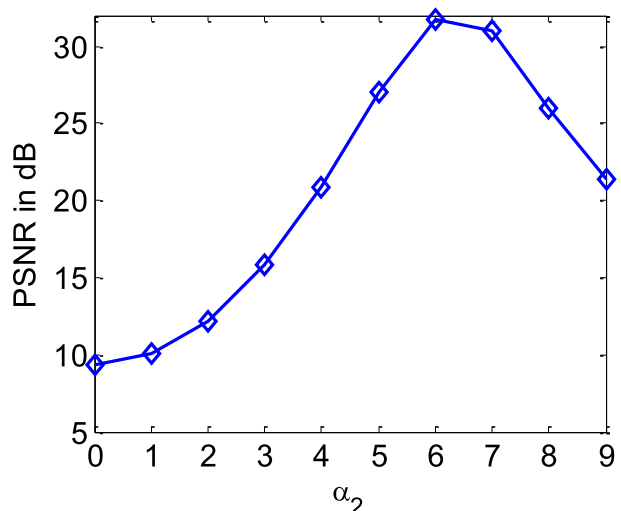


Fig. 5. PSNR versus α_2 in the proposed method using Fly Eye image with $W = 3$, $\alpha_1 = 5$ and $p = 30\%$ ($p_1 = 10\%$, $p_2 = 20\%$).

The relative weights of these components can be controlled by the positive constants α , β , and γ . Typical values of these constants are $\alpha = \beta = \gamma = 1$. The three components are defined as

$$l(x, y) = \frac{2\mu_x\mu_y + C_1}{\mu_x^2 + \mu_y^2 + C_1} \quad (14)$$

$$c(x, y) = \frac{2\sigma_x\sigma_y + C_2}{\sigma_x^2 + \sigma_y^2 + C_2} \quad (15)$$

$$s(x, y) = \frac{\sigma_{xy} + C_3}{\sigma_x\sigma_y + C_3} \quad (16)$$

where μ_x and μ_y are the means of the two images, σ_x and σ_y are their standard deviations, and σ_{xy} is their covariance. The constants C_1 , C_2 , and C_3 are introduced in the fractional expressions of these components to avoid dividing by zero.

The SSIM index represents the arithmetic average of all the SSIM indices computed locally over sliding windows throughout the entire image.

III. SIMULATION RESULTS

The simulations of the proposed method are performed in MATLAB 7.13 (R2011b) on a computer equipped with 2.5-GHz CPU and 6-GB RAM. Six images of different features and sizes have been used in this paper: (512 × 512) *Lena* image, (512 × 512) *bridge* image, (785 × 732) *woman* image, (256 × 256) *mandrill* image, and two microscopic images: (249 × 202) *mammogram* (UPMC, Mammography images, [21]), and (441 × 650) *compound eye of fly* (Scott Robinson, Beckman Institute, University of Illinois at Urbana-Champaign, [22]). These noise-free images are shown in Fig. 1.

Tables I and II show MAE and PSNR of the proposed method using several images corrupted by three different noise densities. The MAE_o and $PSNR_o$ are the MAE and PSNR of the corrupted images before applying any restoration procedure. In contrast to the SSIM, which measures the similarity between the restored image using the proposed method and the original uncorrupted image, the $SSIM_o$ measures the similarity

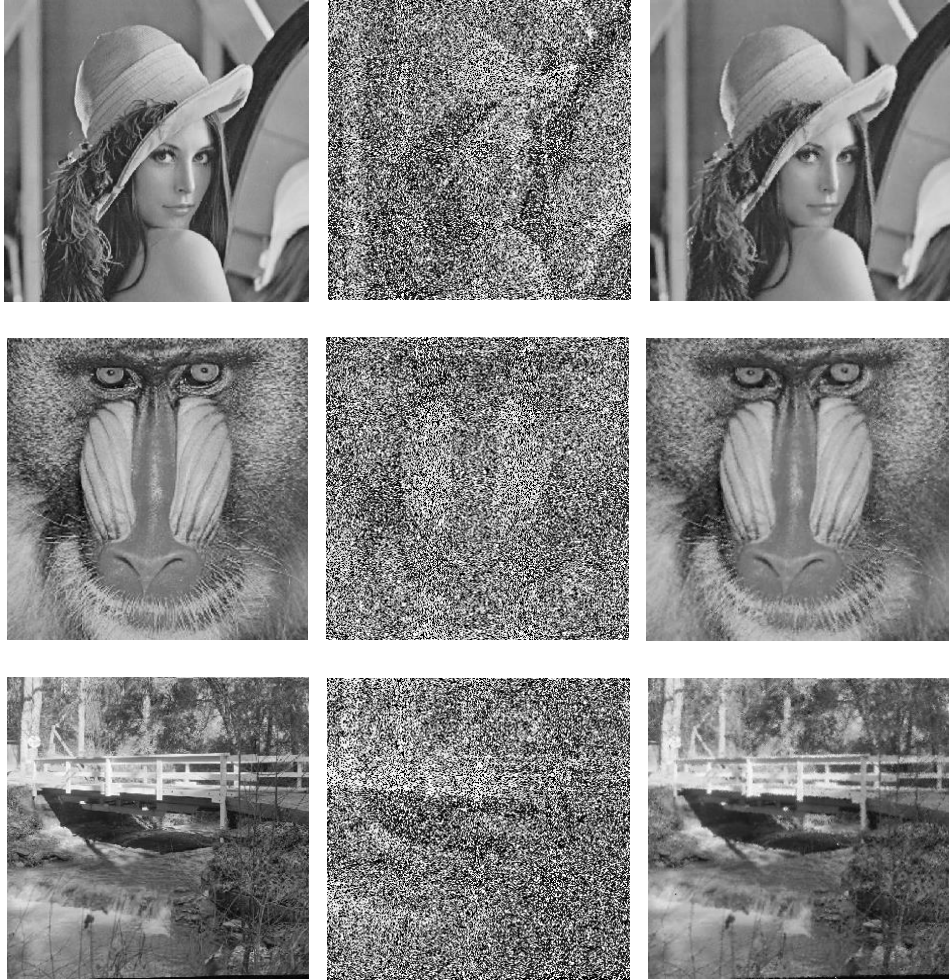


Fig. 6. *Lena*, *Mandrill*, and *bridge* tested images. From left to right: noise-free, corrupted by $p = 60\%$, and restored images using the proposed method.



Fig. 7. Left: *Lena* image corrupted by $p_1 = 20\%$, $p_2 = 40\%$ ($p = 60\%$). Right: restored image using the proposed method.

between the same restored image and the corrupted image before restoration.

Tables I and II use noise models 1 and 2, respectively, both with $m = 4$. These two tables show clearly the significant importance of the two thresholds in the proposed restoration method to produce the best image quality in terms of

quantitative measuring indices. Whether the corrupted image has less or more salt than pepper noise as shown in Table II, the availability of adapting the values of the two thresholds make it possible to get superior results in either case.

The dependency of the PSNR on these threshold values is shown in Figs. 2–5 using noise model 2 for Mammogram



Fig. 8. Left: *Lena* image corrupted by $p_1 = 40\%$, $p_2 = 20\%$ ($p = 60\%$). Right: restored image using the proposed method.

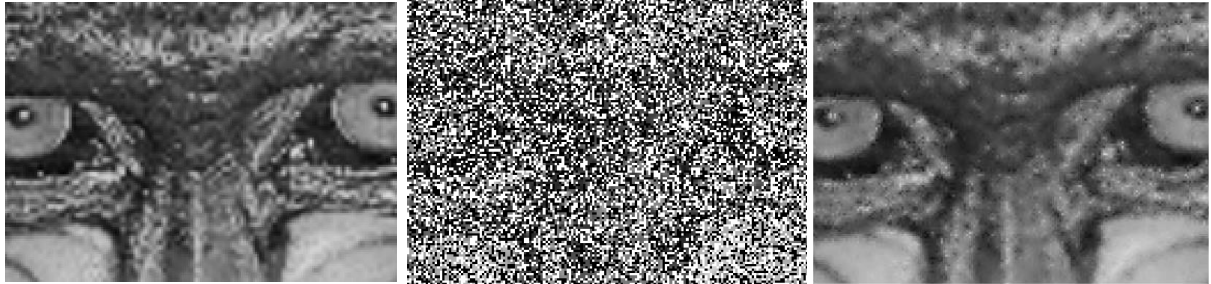


Fig. 9. Left: small part of noise-free Mandrill image. Middle: same part while being corrupted by $p = 60\%$. Right: same part restored using the proposed method.

TABLE III

SUPERIORITY OF THE PROPOSED METHOD OVER SMF WITH DIFFERENT WINDOW SIZES USING VARIOUS PEPPER AND SALT DENSITIES

Method	Noise Density			Lena	Bridge	Mammogram	Fly Eye
	p_1	p_2	p	PSNR	PSNR	PSNR	PSNR
SMF 5×5	20%	40%	60%	13.22	12.36	9.51	10.51
	40%	20%	60%	13.45	13.39	17.27	15.22
	30%	30%	60%	18.64	17.49	17.19	17.53
SMF 7×7	20%	40%	60%	15.53	14.38	12.20	12.98
	40%	20%	60%	15.39	14.93	18.03	16.28
	30%	30%	60%	22.00	19.90	21.07	20.74
SMF 9×9	20%	40%	60%	17.48	15.97	15.16	14.94
	40%	20%	60%	16.92	15.95	18.26	16.62
	30%	30%	60%	21.22	19.83	20.89	20.40
SMF 11×11	20%	40%	60%	18.66	16.91	17.66	16.15
	40%	20%	60%	17.49	16.35	18.00	16.35
	30%	30%	60%	21.23	19.36	20.36	19.67
Proposed 5×5	20%	40%	60%	30.83	25.56	28.32	26.25
	40%	20%	60%	30.81	25.75	28.04	26.34
	30%	30%	60%	30.86	25.59	27.89	26.31

and Fly Eye images corrupted by a noise with $p_2 = 30\%$ ($p_1 = 10\%$, $p_2 = 20\%$).

An optimum value of one value is fixed, and then a plot of PSNR versus the second threshold is depicted in each of

these figures. The maximum values of PSNR indicate the most optimum values of the thresholds to be used in the proposed method. For illustration of the visual appearance of the restored images, Fig. 6 shows three tested imaged

TABLE IV
PSNR (IN dB) AND MAE OF THE PROPOSED METHOD COMPARED WITH OTHER METHODS USING
THREE BENCHMARK IMAGES EACH CORRUPTED BY IMPULSE NOISE WITH $p = 20\%$

<i>Method</i>	Lena		Mandrill		Bridge	
	<i>PSNR</i>	<i>MAE</i>	<i>PSNR</i>	<i>MAE</i>	<i>PSNR</i>	<i>MAE</i>
None	12.54	25.15	12.70	25.16	12.42	25.19
SMF (3×3)	28.88	3.53	26.24	6.47	24.89	7.82
SMF (5×5)	28.84	4.41	23.81	10.42	23.90	10.21
PSM	30.91	3.86	27.05	5.43	27.53	3.74
ATM	37.45	1.71	32.92	2.11	29.43	2.98
FID	37.62	1.63	33.47	2.00	30.19	2.99
CFM	32.81	2.81	29.74	3.15	29.82	2.98
ACWM	36.54	2.13	31.76	2.45	29.14	3.01
DRID	36.22	2.17	31.71	2.36	28.87	3.06
DBA	34.03	2.74	30.11	3.13	27.67	3.62
CD-SMF	30.97	3.99	24.50	9.19	26.12	5.46
MAV	34.32	2.55	30.45	2.76	28.04	3.38
Proposed (3×3)	39.28	0.76	35.22	1.32	32.71	1.77

TABLE V
PSNR (IN dB) OF THE PROPOSED METHOD COMPARED WITH OTHER METHODS USING *Lena*
IMAGE CORRUPTED BY A WIDE RANGE OF NOISE DENSITY FROM $p = 10\%$ TO 60%

<i>Method</i>	<i>Noise Density, p</i>					
	10%	20%	30%	40%	50%	60%
None	15.56	12.54	10.76	9.51	8.55	7.75
SMF	32.95	28.88	27.17	25.52	23.67	21.96
PSM	32.65	30.91	27.50	28.02	23.95	22.91
ATM	41.56	37.42	34.47	31.10	27.03	23.21
FID	41.66	37.55	33.97	30.50	26.46	22.61
CFM	35.14	32.81	30.42	29.51	28.15	25.64
ACWM	41.00	36.54	33.80	31.02	28.27	25.59
DRID	39.11	36.22	33.92	32.15	29.94	27.53
DBA	38.88	34.03	32.60	31.24	29.51	27.67
CD-SMF	32.94	30.97	29.62	27.83	26.00	22.55
MAV	39.09	34.32	32.00	30.27	28.54	27.33
Proposed	42.62	39.29	37.16	34.42	31.91	30.86

before being corrupted (noise free), while being corrupted by $p = 60\%$ impulsive noise, and the restored output images using the proposed method. Despite this large noise level, the restored images are very satisfactory.

Figs. 7 and 8 show the performance of the proposed method using salt and pepper noise with different densities. Fig. 7 shows the *Lena* image corrupted by salt noise more than pepper noise, and the corresponding restored output image using the proposed method. In particular, the image is corrupted by noise of $p_1 = 20\%$ and $p_2 = 40\%$ (i.e., $p = 60\%$). Fig. 8 is similar to Fig. 7 except that the image is corrupted by more pepper noise than salt noise ($p_1 = 40\%$, $p_2 = 20\%$).

A restored small part of *Mandrill* image after being corrupted by noise of $p = 60\%$ is also shown in Fig. 9. Besides noise removal, fine details and edges are still preserved as shown in this figure even with this large noise percentage.

Table III shows a comparison between the proposed method and the SMF method [1] using different window sizes ($W \times W$), and a noise density $p = 60\%$. The comparison shows significant superiority of the proposed method over the SMF method mainly in the case where pepper and salt noise densities are different. Table III shows that the performance of the proposed method is almost the same for different pepper and salt densities as long as the total density is the same.

The two thresholds in the detection step of the proposed algorithm are adapted to keep producing superior performance regardless of whether pepper noise is less or more than the salt noise.

For more extensive analysis of the proposed method, it is compared with a list of several well-known median-based filtering methods as shown in Table IV, namely SMF using different window sizes [1], PSM [5], ATM [6], FID [8], CFM [9], ACWM [10], DRID [12], DBA [13], CD-SMF [14], and MAV [15]. The images used in this comparison are some of benchmark images, which are commonly used in the literature of digital image restoration.

Table V shows the superiority of the proposed method over other state-of-the-art methods using a wide range of impulse noise densities from $p = 10\%$ to 60% . For the SMF method, $W = 3$ is used for $p = 10\%$ and $p = 20\%$, $W = 5$ for $p = 30\%$ and $p = 40\%$, and $W = 7$ for $p = 50\%$ and 60% .

IV. CONCLUSION

In this paper, a new technique for impulsive noise detection and suppression in images has been described and analyzed. Two impulsive noise models applied on several images of different characteristics, and a wide range of noise densities were considered in this paper. Equal and unequal amounts of pepper and salt densities are both considered and examined in this paper. Small sizes of square filtering windows used in the proposed method decrease the blurring problem while preserving image details. Extensive simulation results indicate the superior performance of the proposed method over other existing state-of-the-art methods in terms of image restoration quality and preservation of image fine details and sharp edges.

REFERENCES

- [1] R. C. Gonzalez, R. E. Woods, and S. L. Eddins, *Digital Image Processing Using MATLAB*. Knoxville, TN, USA: Gatesmark Publishing, 2009.
- [2] A. C. Bovic, *The Essential Guide to Image Processing*. New York, NY, USA: Academic, 2009.
- [3] S. J. Ko and Y. H. Lee, "Center weighted median filters and their applications to image enhancement," *IEEE Trans. Circuits Syst.*, vol. 38, no. 9, pp. 984–993, Sep. 1991.
- [4] T. Chen, K. K. Ma, and L. H. Chen, "Tri-state median filter for image denoising," *IEEE Trans. Image Process.*, vol. 8, no. 12, pp. 1834–1838, Dec. 1999.
- [5] Z. Wang and D. Zhang, "Progressive switching median filter for the removal of impulse noise from highly corrupted images," *IEEE Trans. Circuits Syst. II, Analog Digital Signal Process.*, vol. 46, no. 1, pp. 78–80, Jan. 1999.
- [6] W. Luo, "An efficient detail-preserving approach for removing impulse noise in images," *IEEE Signal Process. Lett.*, vol. 13, no. 7, pp. 413–417, Jul. 2006.
- [7] C. C. Kang and W. J. Wang, "Modified switching median filter with one more noise detector for impulse noise removal," *Int. J. Electron. Commun.*, vol. 63, no. 11, pp. 998–1004, 2009.
- [8] W. Luo, "Efficient removal of impulse noise from digital images," *IEEE Trans. Consum. Electron.*, vol. 52, no. 2, pp. 523–527, May 2006.
- [9] M. Nikolova, "A variational approach to remove outliers and impulse noise," *J. Math. Imag. Vis.*, vol. 20, nos. 1–2, pp. 99–120, 2004.
- [10] T. Chen and H. R. Wu, "Adaptive impulse detection using center-weighted median filters," *IEEE Signal Process. Lett.*, vol. 8, no. 1, pp. 1–3, Jan. 2001.
- [11] R. Chan, C. Ho, and M. Nikolova, "Salt-and-pepper noise removal by median-type noise detector and edge-preserving regularization," *IEEE Trans. Image Process.*, vol. 14, no. 10, pp. 1479–1485, Oct. 2005.
- [12] I. Aizenberg and C. Butakoff, "Effective impulse detector based on rank-order criteria," *IEEE Signal Process. Lett.*, vol. 11, no. 3, pp. 363–366, Mar. 2004.
- [13] K. S. Srinivasan and D. Ebenezer, "A new fast and efficient decision based algorithm for removal of high-density impulse noises," *IEEE Signal Process. Lett.*, vol. 14, no. 3, pp. 189–192, Mar. 2007.
- [14] S. Zhang and M. A. Karim, "A new impulse detector for switching median filters," *IEEE Signal Process. Lett.*, vol. 9, no. 11, pp. 360–363, Nov. 2002.
- [15] S. Wang and C. Wu, "A new impulse detection and filtering method for removal of wide range impulse noises," *Pattern Recognit.*, vol. 42, no. 9, pp. 2194–2202, 2009.
- [16] P. Ng and K. Ma, "A switching median filter with boundary discriminative noise detection for extremely corrupted images," *IEEE Trans. Image Process.*, vol. 15, no. 6, pp. 1506–1516, Jun. 2006.
- [17] Z. Wang, A. C. Bovik, H. R. Sheikh, and E. P. Simoncelli, "Image quality assessment: From error visibility to structural similarity," *IEEE Trans. Image Process.*, vol. 13, no. 4, pp. 600–612, Apr. 2004.
- [18] Z. Wang, L. Lu, and A. C. Bovik, "Video quality assessment based on structural distortion measurement," *Signal Process., Image Commun.*, vol. 19, no. 1, pp. 121–132, 2004.
- [19] Z. Wang and A. C. Bovik, "A universal image quality index," *IEEE Signal Process. Lett.*, vol. 9, no. 3, pp. 81–84, Mar. 2002.
- [20] Z. Wang, E. P. Simoncelli, and A. C. Bovik, "Multi-scale structural similarity for image quality assessment," in *Proc. IEEE Asilomar Conf. Signals, Syst. Comput.*, vol. 2, Nov. 2003, pp. 1398–1402.
- [21] (2013, Sep. 10). *Mammography Images*, UPMC, Pittsburgh, PA, USA [Online]. Available: <http://www.upmc.com/services/imaging/services/women/services/breast/pages/mammogram.aspx>
- [22] S. Robinson. (2013, Sep. 10). *Beckman Institute for Advanced Science and Technology* [Online]. Available: <http://itg.beckman.illinois.edu/gallery/2000-06-22.43>



Zayed M. Ramadan (S'02–M'05) received the M.S. and Ph.D. degrees in electrical engineering from the University of Alabama in Huntsville, Huntsville, AL, USA, and the B.S. and M.S. degrees in electrical engineering from the Jordan University of Science and Technology, Irbid, Jordan.

He has been involved with several universities in USA, Dubai, and Saudi Arabia. He is currently with the Electrical and Computer Engineering Department, King Abdulaziz University—North Jeddah Campus, Jeddah, Saudi Arabia. He has authored many publications in peer-reviewed journals and coauthored a textbook on adaptive filtering with MATLAB. His current research interests include digital signal and image processing and their applications, mainly, adaptive filtering and image identification and restoration.